The source of the steep plasma density gradient in middle latitudes during the 11–12 April 2001 storm

S. Park,[1] K.-H. Kim,[1] H. Kil,[2] G. Jee,[3] D.-H. Lee,[1] and J. Goldstein[4]

Received 7 November 2011; revised 20 February 2012; accepted 29 March 2012; published 15 May 2012.

[1] A steep plasma density gradient has been observed in the middle-latitude *F* region during large geomagnetic storms. This phenomenon can be understood as a special form of the middle-latitude ionization trough (hereafter trough), but its causal linkage has not yet been clarified. We investigate the association of the steep density gradient and the trough by comparing their morphologies and occurrence locations using the satellite and ground observation data during the 11–12 April 2001 storm. Steep density gradients are detected in the dusk sector at the equatorward edges of the aurora by the Defense Meteorological Satellite Program (DMSP) F13 spacecraft. The locations of the steep density gradients coincide with the locations of the ionospheric footprints of the plasmapause identified by the Imager for Magnetopause-to-Aurora Global Exploration satellite. These observations demonstrate that the steep density gradient is created at the typical location of the trough. However, the steep density gradient is not produced by the formation of an intense trough during the storm. The temporal evolution of the total electron content maps shows that the steep density gradient observed at dusk by DMSP is associated with the plasma density enhancement in the dayside and its corotation into the dusk sector. The severe plasma density enhancement in middle latitudes, in combination with the trough and presumably the plasma depletion in high latitudes by the neutral composition change, produces the steep density gradient in the subauroral region during the storm.

Citation: Park, S., K.-H. Kim, H. Kil, G. Jee, D.-H. Lee, and J. Goldstein (2012), The source of the steep plasma density gradient in middle latitudes during the 11–12 April 2001 storm, *J. Geophys. Res.*, *117*, A05313, doi:10.1029/2011JA017349.

1. Introduction

[2] The middle-latitude ionization trough (hereafter trough) is a region of reduced plasma density located at the equatorward edge of the auroral oval. The trough is a few degrees wide in latitude and is extended azimuthally [*Moffett and Quegan*, 1983; *Rodger et al.*, 1992; *Lee et al.*, 2011]. Intense troughs develop in the nightside, but the trough is also a dayside phenomenon [*Pryse et al.*, 1998]. Because the trough is primarily a nighttime phenomenon, the extent and severity of the trough are variable with the season. The trough is seen more frequently, extends further toward dawn and dusk, and is more intense during winter than during summer [e.g., *Lee et al.*, 2011]. The trough morphology shows a gradual density variation at the trough's equatorward edge and a sharp density change at the trough's poleward edge. The sharp density change at the trough's poleward edge is explained by the plasma density enhancement on the auroral oval induced by the energetic particle precipitation and transport of dayside plasma [*Rodger et al.*, 1992]. The trough structure appears more complex in the Southern Hemisphere than in the Northern Hemisphere because of the effect of the Weddell Sea anomaly [*Lee et al.*, 2011].

[3] The creation of the trough is explained by the stagnation of plasma flow in the darkness [*Knudsen*, 1974; *Spiro et al.*, 1978]. The horizontal plasma flow in the ionosphere is largely divided into two regions depending on the source: high-latitude convection region and corotation region. The high-latitude convection region is a region where the plasma flow is controlled by the external electric fields (solar wind and magnetospheric electric fields). The two-cell pattern plasma flow in high latitudes is produced by an antisunward flow across the polar cap induced by the solar wind–driven electric field and a sunward flow in the auroral oval induced by the magnetosphere-driven electric field [*Heelis and Hanson*, 1980]. In lower latitudes, plasmas in the ionosphere and

[1]School of Space Research, Kyung Hee University, Gyeonggi, South Korea.
[2]Johns Hopkins University Applied Physics Laboratory, Laurel, Maryland, USA.
[3]Division of Polar Climate Sciences, Korea Polar Research Institute, Incheon, South Korea.
[4]Space Science and Engineering Division, Southwest Research Institute, San Antonio, Texas, USA.

Corresponding author: K.-H. Kim, School of Space Research, Kyung Hee University, 1 Seocheon-dong, Giheung-gu, Yongin-si, Gyeonggi-do 446-701, South Korea. (khan@khu.ac.kr)

0148-0227/12/2011JA017349

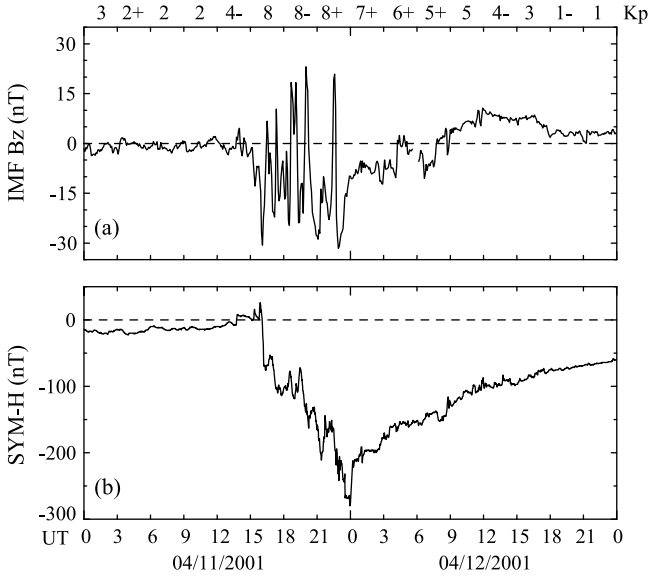

Figure 1. (a) IMF B_z. (b) *SYM-H* index during 11–12 April 2001.

plasmasphere corotate with the Earth by the corotation electric field [*Kelley*, 1989]. In the inertial (or nonrotating) reference frame, the westward plasma flow in the auroral oval and the eastward plasma flow in the corotation region are in opposite directions at premidnight [*Spiro et al.*, 1978]. As a result, the plasma flow is stagnant at the subauroral region. When the plasma flow is stagnant in darkness, this situation provides a longer period for the loss of O^+ by the dissociative recombination with N_2 and O_2 and causes the plasma depletion. The plasma loss by the stagnation is not efficient in the sunlit side because the plasma loss by the stagnant flow is compensated by photoionization. Thus, the trough is more frequently seen and more intense during winter than during summer [e.g., *Lee et al.*, 2011]. The coincidence of the locations of the trough and plasmapause [*Yizengaw and Moldwin*, 2005] supports the idea that the trough is created in association with the stagnant flow. The recent study by *He et al.* [2011] suggested that the trough intensity can be affected by the modulation of the *F* region height by horizontal neutral wind. Because the magnetic declination varies with longitude and the neutral wind effect depends on the magnetic declination, there exists longitudinal variation of the trough intensity [*He et al.*, 2011].

[4] The trough minimum position during solar minimum period experiences the high-low-high latitudinal shift with magnetic local time (MLT), especially for the lower geomagnetic activity level [*Krankowski et al.*, 2009; *Lee et al.*, 2011; *Moffett and Quegan*, 1983; *Muldrew*, 1965; *Weber et al.*, 1985; *Werner and Prölss*, 1997]. Under higher geomagnetic activity conditions, the expansion of the auroral oval and the frictional heating by the subauroral polarization stream (SAPS) (enhanced sunward flow exceeding 1000 m/s at the equatorward edge of auroral particle precipitation [*Foster and Burke*, 2002; *Lee et al.*, 2011; *Rodger et al.*, 1992; *Spiro et al.*, 1979]) create a trough with a narrow latitudinal width and clear poleward edge [*Köhnlein and Raitt*, 1977; *Lee et al.*, 2011; *Muldrew*, 1965].

[5] The most significant change in the trough during storm periods is the equatorward movement of the trough location. This behavior is expected because the high-latitude convection region expands and the plasmasphere shrinks during geomagnetic storms. The trough morphology during storm periods is affected by the changes in the ionosphere and thermosphere. For example, the increase of the velocity difference between the ions and neutrals by a phenomenon such as SAPS increases the reaction rate of O^+ and molecular gases and promotes O^+ loss [*Foster and Vo*, 2002; *Schunk et al.*, 1975]. Energetic particle precipitation may increase the ionization at the poleward edge of the trough, but at the same time, the increased Joule heating on the auroral oval causes an expansion of the atmosphere and promotes O^+ loss by the dissociative recombination with molecular gases. Plasma transport by the intensified horizontal convection further complicates the trough morphology during storm periods.

[6] A steep plasma density gradient (hereafter steep density gradient) has been observed in the subauroral region during large geomagnetic storms [*Heelis and Coley*, 2007; *Kil et al.*, 2011; *Tsurutani et al.*, 2004].This phenomenon can be understood as a special form of the trough [*Tsurutani et al.*, 2004]. However, *Kil et al.* [2011] pointed out that the steep density gradient is not produced by the intensification of the trough during storms and suggested that the steep density gradient observed at dusk or premidnight is associated with the corotation of the severe plasma density enhancement created in the dayside.

[7] This study investigates the source of the steep density gradient by examining its morphology and occurrence location using the observation data during the 11–12 April 2001 storm. The morphology of the steep density gradient and its occurrence latitude are examined by using the measurements of the ion density from the Special Sensor Ionospheric Plasma Drift/Scintillation Meter (SSIES) on board the Defense Meteorological Satellite Program (DMSP) F13 satellite. The location of the auroral oval is inferred from the energy flux data provided by the Special Sensor for Precipitating Particles version 4 (SSJ4) on board the F13 satellite. The ionospheric footprints of the plasmapause are derived by using the plasmasphere data from the Extreme Ultraviolet Imager (EUV) on board the Imager for Magnetopause-to-Aurora Global Exploration (IMAGE) satellite. The temporal and spatial evolution of the ionospheric disturbances is monitored by using the Global Positioning System (GPS) total electron content (TEC) maps.

2. Storm Description

[8] Figures 1a and 1b show the interplanetary magnetic field (IMF) B_z in geocentric solar magnetospheric (GSM) coordinates and the midlatitude *SYM-H* geomagnetic indices [*Iyemori and Rao*, 1996], respectively, during the period 11–12 April 2001. The IMF data were acquired by the Advanced Composition Explorer (ACE) spacecraft [*Stone et al.*, 1998], and the *SYM-H* index was obtained from the World Data Center at Kyoto University. During the storm period, ACE was located near (221, 2, −21) R_E in GSM coordinates. On the top of Figure 1a, the 3 h values of the *Kp* index are shown. The IMF data are presented after

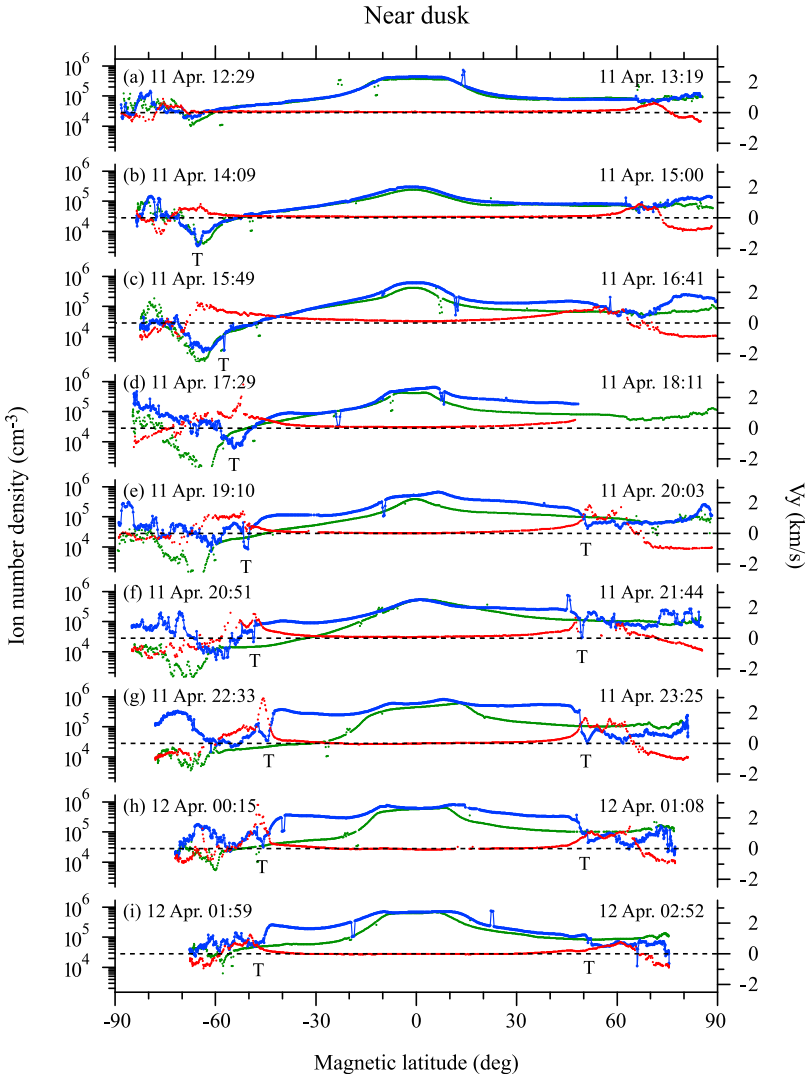

Figure 2. Measurements of the ion density and ion velocity (V_y component) near 1800 LT by DMSP F13. The plasma density measurements on 11–12 and 10–11 April are shown with blue and green curves, respectively. The ion velocity is shown with red curves. The trough locations are denoted with a letter T. The UT on each plot is the beginning time of each orbit.

the time was shifted to the location of the bow shock nose. The IMF data were provided in 5 min time resolution. The middle-latitude *SYM-H* geomagnetic index has a time resolution of 1 min. The *SYM-H* geomagnetic index is essentially the same as the hourly *Dst* index, which is the crude indicator of the equatorial magnetic perturbations associated with the storm time ring current.

[9] Before ~1500 UT on 11 April 2001, the IMF B_z component shows a minor fluctuation. After 1500 UT, the IMF B_z component shows fluctuations with an amplitude more than 30 nT. Although several intervals of the northward IMF exist, the southward IMF is dominant during the main and early recovery phases of the storm. The 1 min *SYM-H* index reaches to −270 nT at 2300 UT and then gradually increases. The main phase of this storm is characterized by extremely disturbed geomagnetic activities with a *Kp* value as large as 8^+. The steep density gradient is detected by F13 at dusk between 2200 and 0200 UT on 11–12 April 2001.

3. Results

[10] We examine the temporal variation of the ionospheric morphology by using the DMSP F13 data. The DMSP satellite orbits are at an altitude of 830 km with a 98° inclination. The ion density and ion velocity are measured by the retarding potential analyzer and the ion drift meter, respectively, in the SSIES package. Figure 2 presents the F13 data for nine consecutive orbits (from the south to the north) at the approximate solar local time of 1800 LT at the equator. The blue and red curves show the ion density and the y component of the ion velocity (V_y), respectively, on 11–12 April. The measurements of the ion density on 10–11 April (green curves) are included as a quiet time reference. The UT given

in the top left of each plot is the beginning time of the orbit. The V_y component is the horizontal ion velocity perpendicular to the satellite pass. For the F13 pass, the positive and negative V_y values correspond to the sunward and antisunward flows, respectively. The velocities are in the rotation frame of the Earth. The trough features on 11–12 April are indicated with a letter "T." In Figure 2e, the trough location in the magnetic south can be either the sharp density drop denoted with a letter T or the broader density depletion located at about 10° higher latitude from the location of T. As we show later, the locations denoted with a letter T agree with the plasmapause locations and are close to the equatorward boundaries of the diffusive aurora. The horizontal plasma flow in Figure 2 also shows that the locations at T are close to the region where the plasma velocity changes significantly, i.e., the corotation boundary. For these reasons, the locations of T are chosen as the trough locations.

[11] We point out four notable changes during the storm period (blue curves in Figures 2d–2i). First, the plasma density is significantly enhanced in middle latitudes during the storm period. The middle-latitude density around 40°S is enhanced by a factor of 10. The steep density gradient is created in the region where the middle-latitude density enhancement is significant (Figures 2g and 2h). Second, the hemispheric asymmetry in plasma density weakens or disappears in low and middle latitudes during the storm period. Although the observations were made just 20 days past the spring equinox, the hemispheric asymmetry in plasma density appears before the storm; the hemispheric asymmetry observed in April is similar to that which occurs during the June solstice [*Kil et al.*, 2006; *West and Heelis*, 1996] and is attributed to the effect of the interhemispheric winds. In addition, the local time difference between the DMSP F13 orbits in the Northern and Southern Hemispheres near the evening terminator causes the hemispheric asymmetry. Since the inclination of the DMSP F13 orbit is about 98°, the spacecraft samples data at a later local time in the Southern Hemisphere than in the Northern Hemisphere with a local time difference of ~2 h between 60°S and 60°N. If the interhemispheric winds were the source of the hemispheric asymmetry before the storm, the disappearance of the hemispheric asymmetry during the storm can be interpreted as an indication of the global wind circulation change by the heating of the polar atmosphere. The density enhancement in the Southern Hemisphere is more pronounced than that in the Northern Hemisphere because the hemispheric asymmetry existed before the storm. Third, the trough feature is seen to be more pronounced before the storm than during the storm. In Figures 2d and 2e, we can identify a development of deep troughs in the magnetic south (between 60°S and 70°S) before the storm (green curves). However, the depth of the trough is reduced with an onset of the storm (blue curves). The development of more intense troughs in the magnetic south than in the magnetic north can be explained by the longitudinal dependence of the deepest trough location and/or the F13 orbit. *He et al.* [2011] reported that the midlatitude deepest trough near midnight (2200–0200 MLT) develops in 15°–75°E in the Southern Hemisphere and in 180°–90°W in the Northern Hemisphere during equinoxes. Although F13 trough observations in our study were done around 1800 MLT, huge density depletion in the Southern Hemisphere compared to the Northern Hemisphere, shown in Figures 2a–2f, would be associated with the large longitudinal difference in the deepest trough location between the Southern and Northern Hemispheres. We note that F13 for the intervals from Figures 2a to 2f passed near the longitudinal region of the deepest trough in the Southern Hemisphere. We also attribute the deep trough in the Southern Hemisphere to F13 orbit. The sampling LT in the southern trough region is ~1900 LT and that in the northern trough region is ~1700 LT. Because the trough feature starts to appear around 1800 LT during equinox [*Lee et al.*, 2011; *He et al.*, 2011], F13 detects a more intense trough in the Southern Hemisphere than in the Northern Hemisphere. Fourth, the trough location moves to lower latitudes as the storm progresses (Figures 2d–2g).

[12] In Figure 3, we examine the trough morphology in some detail with the F13 observations at two time intervals, 1730–1812 UT and 2233–2325 UT. The observations in Figures 3a, 3c, and 3e were made just after the storm onset, and the observations in Figures 3b, 3d, and 3f were made near the end of the main phase. Figures 3a and 3b show the measurements of the ion density (blue curve) and V_y (red curve). The electron and ion energy fluxes observed by F13/SSJ4 are shown in Figures 3c and 3d and Figures 3e and 3f, respectively. The location of the auroral oval is identified by the region of the enhanced energy flux. The equatorward boundaries of the diffuse aurora are denoted with the vertical dashed lines. In Figure 3a, a typical trough feature appears at the equatorward auroral edge. A spike-like sunward flow is detected near the center of the trough, and it may be interpreted as the SAPS [*Foster and Vo*, 2002]. The SAPS (indicated with a letter "S") also appears in Figure 3b.

[13] By comparing the density plots in Figures 3a and 3b, we can identify the fact that the creation of the steep density gradient (Figure 3b) is not related to the creation of a deep trough in the subauroral region. We can identify only weak signatures of the trough in the subauroral region in Figure 3b, although the trough is clearly visible in Figure 3a. The creation of the steep density gradient in both the magnetic south and north in Figure 3b is related to the plasma density enhancement in middle latitudes and a sudden density drop in the aurora oval. The steep density gradient is created in the region where the plasma velocity changes significantly, and therefore, plasma convection can be considered as a plausible source of the steep density gradient. However, the plasma density does not show a good correlation with the horizontal plasma flow velocity. In the magnetic north in Figure 3b, we observe the sunward flow in the auroral oval (1.6 km/s) and antisunward flow in the polar cap (−1 km/s), but the plasma density shows only a minor fluctuation across the auroral oval and polar cap. In Figure 3b, the locations of the SAPS and the steep density gradient coincide in both hemispheres. However, the SAPS itself does not seem to create the steep density gradient: the steep density gradient appears in Figure 3b, but it does not in Figure 3a, although the SAPS features in the Southern Hemisphere in Figures 3a and 3b are similar.

[14] The steep density gradient detected by F13 is not considered to be created instantaneously at dusk because the plasma density change is caused by a cumulative ionospheric response to the storm. We track the development history of the steep density gradient by using TEC maps. We use the TEC maps in the magnetic north because the GPS

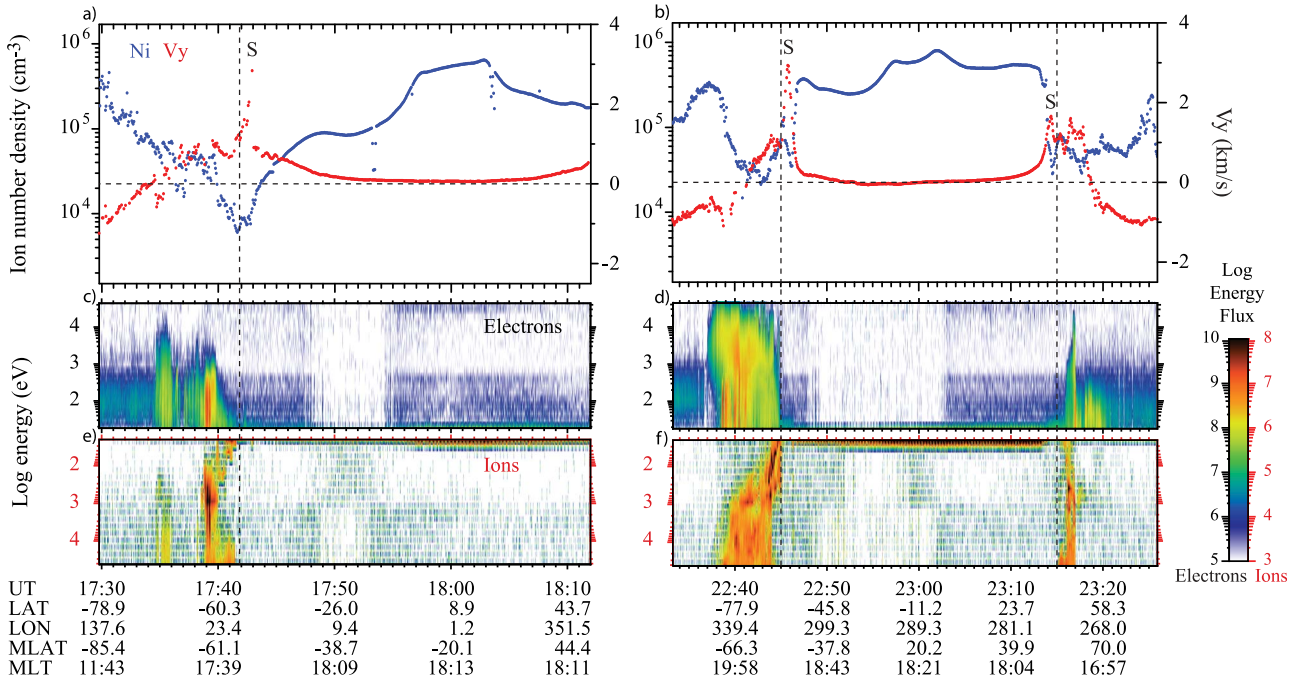

Figure 3. Measurements of the ion density and V_y component by F13/SSIES and electron and ion energy flux measured by F13/SSJ4 at (a, c, e) 1730–1812 UT on 11 April (at the beginning of the main phase) and (b, d, f) 2233–2325 UT on 11 April (at the end of the main phase). The SAPS features are denoted with a letter S.

station is distributed more densely in the Northern Hemisphere than in the Southern Hemisphere. Figure 4 shows the TEC maps at 1300, 1700, and 2300 UT on 11 April in the MLT and magnetic latitude frame. The plots of the F13 data below the TEC maps are the same format as Figure 3. The F13 pass is close to the dusk-to-dawn line. The TEC map at 1300 UT is representative of the ionosphere before the storm. At 1700 UT, significant TEC enhancements, compared to the TEC before the storm, appear in middle latitudes in the dayside. However, the TEC change in the dusk and premidnight sectors is relatively small. The steep density gradient does not appear at this time in the F13 data. In comparison of the TEC maps at 1700 and 2300 UT, we observe the rotation of the dayside TEC enhancement into the dusk and premidnight sectors. The TEC morphology at 2300 UT is consistent with the F13 observation of the severe density enhancement in middle latitudes in the dusk sector. The TEC maps show that the steep density gradient has already existed at 1700 UT in the American sector (marked by an oval) when this sector was in the noon sector. It takes about 6 h for the steep density gradient created in the noon sector to corotate into the dusk sector, and F13 detects the steep density gradient in the dusk sector at 2300 UT. The sunward plasma convection in the auroral oval and the antisunward convection in the polar cap are intensified at both 1700 and 2300 UT compared to those before the storm, but the steep density gradient appears only at 2300 UT. This observation indicates that the creation of the steep density gradient is not directly related to the plasma flow.

[15] The DMSP F13 observations show that the steep density gradient is created at the subauroral region where the trough develops. To verify the development of the steep density gradient at the trough locations, we infer the trough locations by using the ionospheric footprint of the plasmapause. Figure 5a shows the *SYM-H* index, Figure 5b shows the magnetic latitudes of the ionospheric footprints of the plasmapause (open circles) and trough (solid circles), and Figures 5c–5f show sample plasmapause maps in the L value and MLT frame at the times indicated in the *SYM-H* index plot. The ionospheric footprints of the plasmapause at 1800 MLT are extracted from the IMAGE/EUV plasmasphere data [*Goldstein and Sandel*, 2005] using the dipole magnetic field model. The trough locations are obtained from the F13 data presented in Figure 2. Data gaps in the extracted plasmapause locations are due to noise or sunlight contamination. Details of instrument artifacts were described by *Goldstein et al.* [2004a]. At 1350 UT (before the storm), the plasmapause shows a clear shape in the night-dawn sectors and is located around $L \approx 3.5$–4.5 (Figure 5c). At 1623 UT (just after the onset of the storm main phase), the plasmapause locations in the nightside move to $L \approx 3$ (Figure 5d). Deducing from the plasmapause location in the morning sector, the noon sector plasmapause is seen to expand outward. In other words, the dayside plasmaspheric plasma is seen to surge sunward, forming a drainage plume in a broad MLT range [*Goldstein et al.*, 2004b; *Spasojević et al.*, 2003]. The simultaneous inward nightside motion and outward dayside motion of the plasmasphere, which is called plasmaspheric erosion, are related to the enhanced sunward plasma convection [*Kim et al.*, 2007]. The snapshots at 2321 and 0235 UT (after hours of the plasmasphere erosion) show a very eroded plasmasphere with the shrink of the dawnside plasmapause location to $L \approx 2$ (Figures 5e and 5f). The plasmasphere tail feature appears in the 1600 MLT sector in Figures 5e and 5f. The locations of the trough at the times of plasmapause snapshots are indicated with open circles.

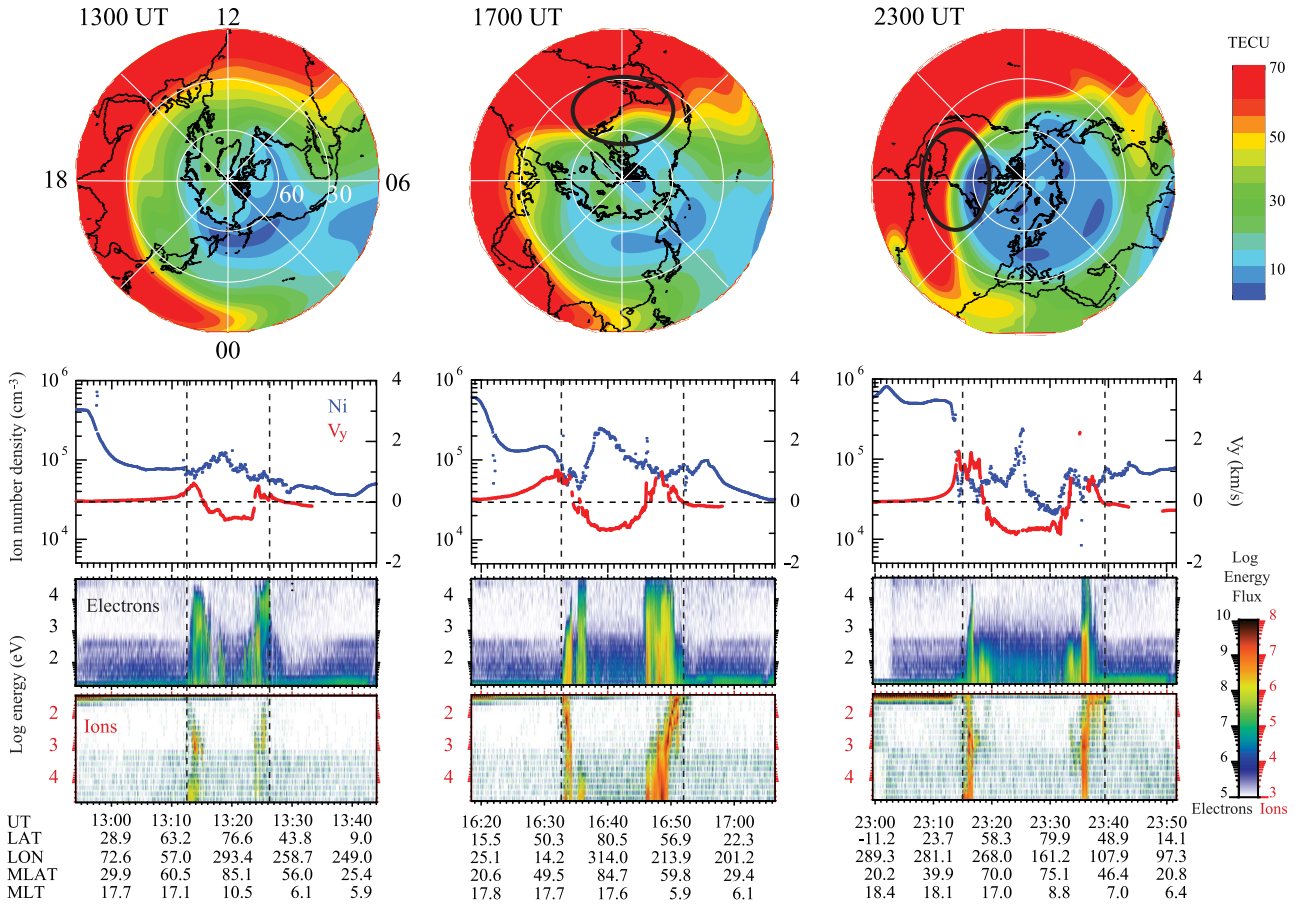

Figure 4. GPS TEC maps in the magnetic north at 1300, 1700, and 2300 UT on 11 April. The F13 observations below each TEC map are the same format as Figure 3.

As Figure 5b shows, the locations of the plasmapause and trough (including the steep density gradient) in the dusk sector show a good agreement; those locations move equatorward as the storm progresses and reach to ±45° magnetic latitudes at the end of the main phase of the storm. These observation results demonstrate that the steep density gradients are created at the typical locations of the trough. *Yizengaw et al.* [2005] identified the coincidence of the ionospheric footprints of the plasmapause and trough by comparison of the IMAGE/EUV plasmasphere and GPS TEC data during the 31 March 2001 storm.

4. Discussion

[16] The storm time steep plasma density gradient in middle latitudes can be understood in terms of the trough because the location of the steep density gradient coincides with the location of the ionospheric footprint of the plasmapause. In addition, the location of the steep density gradient at a fixed local time appears to move in latitude following the storm phase [*Heelis and Coley*, 2007; *Tsurutani et al.*, 2004]. This storm-phase-dependent movement is similar to the storm-phase-dependent movement of the ionospheric footprint of the plasmapause. However, the temporal evolution of the TEC maps shows that the apparent storm-phase-dependent movement of the steep density gradient location can also be caused by the corotation of the density gradient whose location is variable with longitude. Both the temporal and spatial variations of the ionosphere should be taken into account to understand the storm time behavior of the steep density gradient phenomenon.

[17] The observation results during the 11–12 April 2001 storm are similar to those during the 20 November 2003 storm reported by *Kil et al.* [2011]. The consistent features during both storms are summarized as follows: (1) Severe plasma density enhancement in middle latitudes occurs near the noon sector during the early main phase of the storm. (2) The plasma density enhancement in the dayside corotates with the Earth. (3) The steep density gradient occurs at the typical latitudes where the trough develops. (4) The steep density gradient is detected at dusk or premidnight in the longitude region where the severe plasma density enhancement occurs when that region was in the dayside. (5) The steep density gradient occurs at dusk or premidnight several hours after the onset of the storm because of the corotation time of the severe plasma density enhancement in the noon sector. (6) The creation of the steep density gradient is not caused by a formation of a deep trough.

[18] The results summarized above suggest that the formation of the steep density gradient is initiated by the plasma density enhancement in the dayside at the early stage of the storm. The plasma density enhancement in the local region is persistent and corotates. As the storm proceeds, the middle-latitude plasma density enhancement is seen to be

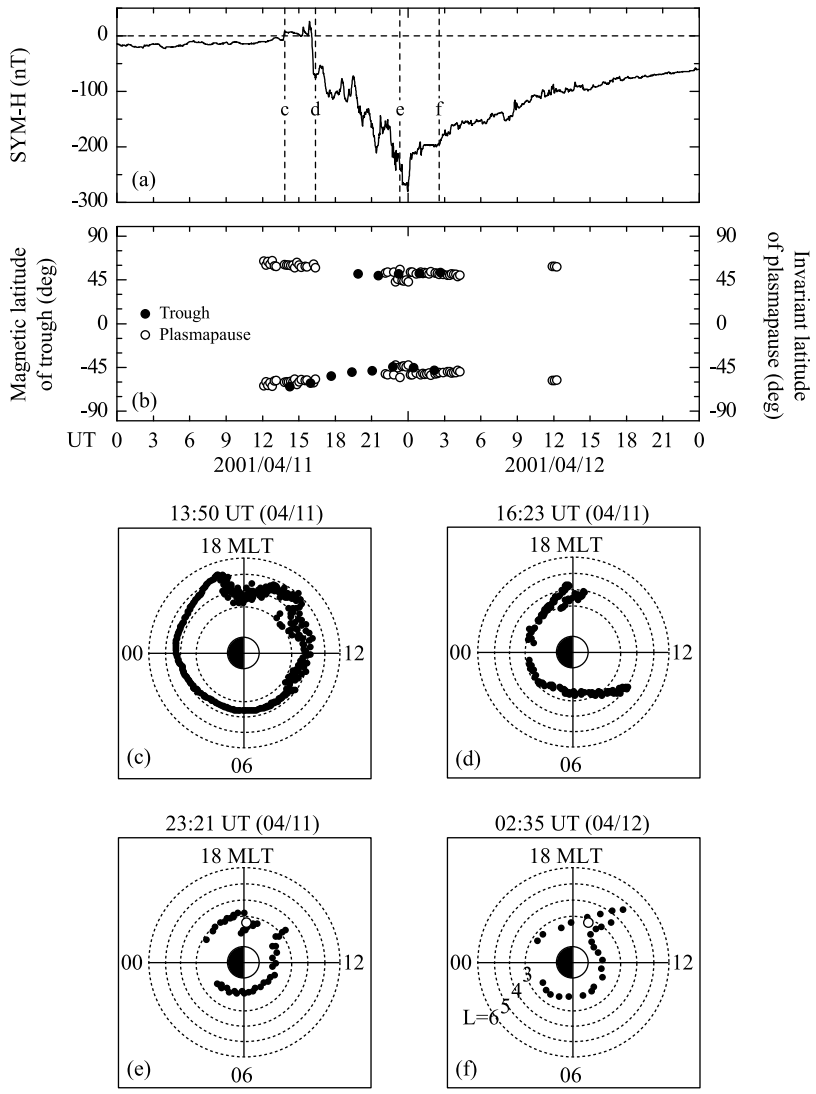

Figure 5. (a) *SYM-H* index. (b) The locations of the trough (solid circles) identified by the F13 plasma density data and of the plasmapause identified by the IMAGE/EUV data (open circles). (c–f) Plasmapause maps in the *L* value MLT frame at 1350, 1623, and 2321 UT on 11 April and at 0235 UT on 12 April derived from the IMAGE/EUV data. In Figures 5e and 5f, the locations of the trough are shown with open circles.

more intensified. The plausible drivers of the plasma density enhancement in low and middle latitudes are the storm-induced eastward electric field and equatorward wind [*Crowley et al.*, 2006; *Kil et al.*, 2007; *Lin et al.*, 2005; *Lu et al.*, 2008; *Mannucci et al.*, 2005; *Prölss*, 1993]. The main phase of the storm lasted for 8 h from ~1600 UT on 11 April to ~0000 UT on 12 April. Thus, storm-induced equatorward wind is assumed to be persistent until ~0000 UT on 12 April. As long as the wind was persistent, the density enhancement would also be persistent. The plasma density enhancement in middle latitudes would act as an obstacle against the equatorward expansion of the polar region thermospheric neutral composition disturbance, and the persistent steep density gradient is formed at that boundary.

[19] The observation of the equatorial ionization anomaly (EIA) feature in Figures 2g and 2h demonstrates the enhancement of the upward plasma drift (or eastward electric field) during the storm period. However, the plasma density enhancement in middle latitudes may not be explained by the effect of the storm-induced upward plasma drift alone. The apex height of the magnetic field at 40° magnetic latitude at an altitude of 830 km is about 6000 km. Diffusion of plasma from such a high altitude cannot produce the middle-latitude plasma density enhancement by a factor of 10. Uplift of the ionosphere by storm-induced equatorward winds may play an important role in the plasma density enhancement in middle latitudes [*Crowley et al.*, 2006;*Kil et al.*, 2003; *Lin et al.*, 2009; *Prölss*, 1993]. In Figure 2f, we observe the plasma density enhancement in middle latitudes during the storm, although the EIA feature does not appear; storm-induced equatorward winds are the plausible source of the density enhancement in middle latitudes. Severe plasma density enhancement in middle latitudes is produced by the

synergistic effect of the storm-induced electric field and winds [*Lin et al.*, 2009].

[20] Assuming that the middle-latitude plasma density enhancement is produced by the storm-induced electric field and neutral winds, why are those effects confined to lower latitudes of the ionospheric footprint of the plasmapause? The steep density gradient is created at the typical location of the trough, and therefore, the formation of the trough contributes to the creation of the steep density gradient during the storm period. However, it should be noted that the steep density gradient is not caused by the creation of an intense trough during the storm. Actually, the trough is less pronounced during the storm than it is before the storm (see Figures 2d–2f). The creation of the steep density gradient by the step-like density change is not explained by the creation of the trough alone. The step-like density change indicates that a plasma density suppression mechanism is effective in high latitudes. In Figure 3b, the creation of the steep density gradient in the magnetic south is associated with the reduction of the plasma density in the auroral region, and the creation of the steep density gradient in the magnetic north is associated with the reduction of the plasma density in the auroral oval and polar cap. The neutral composition change is the plausible plasma density suppression mechanism on the auroral oval and polar cap [e.g., *Fuller-Rowell et al.*, 1996; *Prölss*, 1995]. Heating of the atmosphere on the auroral oval and polar cap induces an expansion of the atmosphere. As a result, the number density of molecular gases increases in the *F* region, and the plasma loss by the dissociative recombination of oxygen ions with molecular gases is promoted. The severe plasma density enhancement in the dayside may interrupt the equatorward expansion of the neutral composition disturbance and confine the neutral composition disturbance within the high-latitude convection region. In Figure 4, the TEC in the auroral oval and polar cap at 2300 UT is smaller than that at 1700 UT. The F13 observations also show that plasma density is reduced during the storm period in high latitudes in the magnetic north. In the TEC plot at 2300 UT in Figure 4, we can identify the extension of the reduced TEC region toward the postmidnight sector. The local time distribution of the TEC reduced region is consistent with the predicted behavior of the neutral composition disturbance; the neutral composition disturbance preferentially expands toward the postmidnight sector [*Prölss*, 1993].

5. Conclusion

[21] We have investigated the relationship between the trough and the steep plasma density gradient in middle latitudes during the 11–12 April 2001 storm. The steep density gradients are detected in the American sector at dusk by DMSP F13. The coincidence of the locations of the steep density gradients and the ionospheric footprints of the plasmapause derived from the IMAGE/EUV data indicates the creation of the steep density gradient at the trough locations. However, the steep density gradient is not created by the creation of an intense trough during the storm. Actually, the trough feature during the storm is less pronounced than it is before the storm. The global TEC maps show that the steep density gradient is initiated by the severe plasma density enhancement in the dayside at the early stage of the storm. The detection of the steep density gradient at dusk by F13 is associated with the corotation of the severe plasma density enhancement in the dayside into the dusk sector. Thus, the major source of the steep density gradient is the middle-latitude plasma density enhancement in the dayside at the beginning of the storm. Formation of the trough and the plasma depletion in the auroral oval presumably by the neutral composition change contribute to the creation of the steep density gradient in the subauroral region.

[22] **Acknowledgments.** H. Kil acknowledges support from the National Science Foundation National Space Weather Program (AGS-1024886). G. Jee acknowledges support from project PP11030 funded by the Korea Polar Research Institute. This work was supported by the WCU program through NRF funded by MEST of Korea (R31-10016). Work of K.-H. Kim was supported by the Basic Science Research Program through NRF funded by MEST of Korea (2010-0007393). The author acknowledges the University of Texas at Dallas for provision of the DMSP data. The key parameter solar wind and magnetic field data of the ACE satellite were provided by NASA's CDAWeb site. The geomagnetic indices (*SYM-H* and *Kp*) were provided by World Data Center C2 (WDC-C2) for Geomagnetism, Kyoto University. The CODE GIMs TEC data were obtained from the Crustal Dynamics Data Information System (CDDIS) at Goddard Space Flight Center, NASA.

[23] Robert Lysak thanks the reviewers for their assistance in evaluating this paper.

References

Crowley, G., et al. (2006), Global thermosphere-ionosphere response to onset of 20 November 2003 magnetic storm, *J. Geophys. Res.*, *111*, A10S18, doi:10.1029/2005JA011518.

Foster, J. C., and W. J. Burke (2002), SAPS: A new characterization for sub-auroral electric fields, *Eos Trans. AGU*, *83*, 393–394.

Foster, J. C., and H. B. Vo (2002), Average characteristics and activity dependence of the subauroral polarization stream, *J. Geophys. Res.*, *107*(A12), 1475, doi:10.1029/2002JA009409.

Fuller-Rowell, T. J., M. V. Codrescu, H. Rishbeth, R. J. Moffett, and S. Quegan (1996), On the seasonal response of the thermosphere and ionosphere to geomagnetic storms, *J. Geophys. Res.*, *101*(A2), 2343–2353.

Goldstein, J., and B. R. Sandel (2005), The global pattern of evolution of plasmaspheric drainage plumes, in *Inner Magnetosphere Interactions: New Perspectives From Imaging*, *Geophys. Monogr. Ser.*, vol. 159, edited by J. L. Burch, M. Schulz, and H. Spence, pp. 1–22, AGU, Washington, D. C., doi:10.1029/159GM02.

Goldstein, J., B. R. Sandel, M. R. Hairston, and S. B. Mende (2004a), Plasmapause undulation of 17 April 2002, *Geophys. Res. Lett.*, *31*, L15801, doi:10.1029/2004GL019959.

Goldstein, J., B. R. Sandel, M. F. Thomsen, M. Spasojević, and P. H. Reiff (2004b), Simultaneous remote sensing and in situ observations of plasmaspheric drainage plumes, *J. Geophys. Res.*, *109*, A03202, doi:10.1029/2003JA010281.

He, M., L. Liu, W. Wan, and B. Zhao (2011), A study on the nighttime midlatitude ionospheric trough, *J. Geophys. Res.*, *116*, A05315, doi:10.1029/2010JA016252.

Heelis, R. A., and W. R. Coley (2007), Variations in the low- and middle-latitude topside ion concentration observed by DMSP during superstorm events, *J. Geophys. Res.*, *112*, A08310, doi:10.1029/2007JA012326.

Heelis, R. A., and W. B. Hanson (1980), High-latitude ion convection in the nighttime *F* region, *J. Geophys. Res.*, *85*(A5), 1995–2002.

Iyemori, T., and D. R. K. Rao (1996), Decay of the Dst field of geomagnetic disturbance after substorm onset and its implication to storm-substorm relation, *Ann. Geophys.*, *14*, 608–618.

Kelley, M. C. (1989), *The Earth's Ionosphere*, Academic, San Diego, Calif.

Kil, H., L. J. Paxton, X. Pi, M. R. Hairston, and Y. Zhang (2003), Case study of the 15 July 2000 magnetic storm effects on the ionosphere-driver of the positive ionospheric storm in the winter hemisphere, *J. Geophys. Res.*, *108*(A11), 1391, doi:10.1029/2002JA009782.

Kil, H., R. DeMajistre, L. J. Paxton, and Y. Zhang (2006), Nighttime F-region morphology in the low and middle latitudes seen from DMSP F15 and TIMED/GUVI, *J. Atmos. Terr. Phys.*, *68*, 1672–1681.

Kil, H., S.-J. Oh, L. J. Paxton, Y. Zhang, S.-Y. Su, and K.-W. Min (2007), Spike-like change of the vertical $\mathbf{E} \times \mathbf{B}$ drift in the equatorial region during very large geomagnetic storms, *Geophys. Res. Lett.*, *34*, L09103, doi:10.1029/2007GL029277.

Kil, H., L. Paxton, K.-H. Kim, S. Park, Y. Zhang, and S.-J. Oh (2011), Temporal and spatial components in the storm-time ionospheric disturbances, *J. Geophys. Res.*, *116*, A11315, doi:10.1029/2011JA016750.

Kim, K.-H., J. Goldstein, and D. Berube (2007), Plasmaspheric drainage plume observed by the Polar satellite in the prenoon sector and the IMAGE satellite during the magnetic storm of 11 April 2001, *J. Geophys. Res.*, *112*, A06237, doi:10.1029/2006JA012030.

Knudsen, W. C. (1974), Magnetospheric convection and the high-latitude F_2 ionosphere, *J. Geophys. Res.*, *79*(7), 1046–1055.

Köhnlein, W., and W. J. Raitt (1977), Position of the midlatitude trough in the topside ionosphere as deduced from ESRO 4 observations, *Planet. Space Sci.*, *25*, 600–602, doi:10.1016/0032-0633(77)90069-1.

Krankowski, A., I. I. Shagimuratov, I. I. Ephishov, A. Krypiak-Gregorczyk, and G. Yakimova (2009), The occurrence of the midlatitude ionospheric trough in GPS-TEC measurements, *Adv. Space Res.*, *43*, 1721–1731, doi:10.1016/j.asr.2008.05.014.

Lee, I. T., W. Wang, J. Y. Liu, C. Y. Chen, and C. H. Lin (2011), The ionospheric midlatitude trough observed by FORMOSAT-3/COSMIC during solar minimum, *J. Geophys. Res.*, *116*, A06311, doi:10.1029/2010JA015544.

Lin, C. H., A. D. Richmond, R. A. Heelis, G. J. Bailey, G. Lu, J. Y. Liu, H. C. Yeh, and S.-Y. Su (2005), Theoretical study of the low- and midlatitude ionospheric electron density enhancement during the October 2003 superstorm: Relative importance of the neutral wind and the electric field, *J. Geophys. Res.*, *110*, A12312, doi:10.1029/2005JA011304.

Lin, C. H., A. D. Richmond, G. J. Bailey, J. Y. Liu, G. Lu, and R. A. Heelis (2009), Neutral wind effect in producing a storm time ionospheric additional layer in the equatorial ionization anomaly region, *J. Geophys. Res.*, *114*, A09306,doi:10.1029/2009JA014050.

Lu, G., L. P. Goncharenko, A. D. Richmond, R. G. Roble, and N. Aponte (2008), A dayside ionospheric positive storm phase driven by neutral winds, *J. Geophys. Res.*, *113*, A08304, doi:10.1029/2007JA012895.

Mannucci, A. J., B. T. Tsurutani, B. A. Iijima, A. Komjathy, A. Saito, W. D. Gonzalez, F. L. Guarnieri, J. U. Kozyra, and R. Skoug (2005), Dayside global ionospheric response to the major interplanetary events of October 29–30, 2003 "Halloween Storms," *Geophys. Res. Lett.*, *32*, L12S02, doi:10.1029/2004GL021467.

Moffett, R. J., and S. Quegan (1983), The mid-latitude trough in the electron concentration of the ionospheric *F*-layer: A review of observations and modelling, *J. Atmos. Terr. Phys.*, *45*, 315–343.

Muldrew, D. B. (1965), F-layer ionization trough deduced from Alouette data, *J. Geophys. Res.*, *70*, 2635–2650, doi:10.1029/JZ070i011p02635.

Prölss, G. W. (1993), On explaining the local time variation of ionospheric storm effects, *Ann. Geophys.*, *11*, 1–9.

Prölss, G. W. (1995), Ionospheric *F* region storms, in *Handbook of Atmospheric Electrodynamics*, edited by H. Volland, pp. 195–248, CRC Press, Boca Raton, Fla.

Pryse, S. E., L. Kersley, M. J. Williams, and I. K. Walker (1998), The spatial structure of the dayside ionospheric trough, *Ann. Geophys.*, *16*, 1169–1179.

Rodger, A. S., R. J. Moffett, and S. Quegan (1992), The role of ion drift in the formation of ionisation troughs in the mid- and high-latitude ionosphere—A review, *J. Atmos. Terr. Phys.*, *54*, 1–30.

Schunk, R. W., W. J. Raitt, and P. M. Banks (1975), Effect of electric fields on the daytime high-latitude *E* and *F* regions, *J. Geophys. Res.*, *80*(22), 3121–3130.

Spasojević, M., J. Goldstein, D. L. Carpenter, U. S. Inan, B. R. Sandel, M. B. Moldwin, and B. W. Reinisch (2003), Global response of the plasmasphere to a geomagnetic disturbance, *J. Geophys. Res.*, *108*(A9), 1340, doi:10.1029/2003JA009987.

Spiro, R. W., R. A. Heelis, and W. B. Hanson (1978), Ion convection and the formation of the mid-latitude *F* region ionization trough, *J. Geophys. Res.*, *83*(A9), 4255–4264.

Spiro, R. W., R. A. Heelis, and W. B. Hanson (1979), Rapid subauroral ion drifts observed by Atmosphere Explorer C, *Geophys. Res. Lett.*, *6*(8), 657–660.

Stone, E. C., A. M. Frandsen, R. A. Mewaldt, E. R. Christian, D. Margolies, J. F. Ormes and F. Snow (1998), The Advanced Composition Explorer, *Space Sci. Rev.*, *86*, 1–22.

Tsurutani, B., et al. (2004), Global dayside ionospheric uplift and enhancement associated with interplanetary electric fields, *J. Geophys. Res.*, *109*, A08302, doi:10.1029/2003JA010342.

Weber, E. J., R. T. Tsunoda, J. Buchau, R. E. Sheehan, D. J. Strickland, W. Whiting, and J. G. Moore (1985), Coordinated measurements of auroral zone plasma enhancements, *J. Geophys. Res.*, *90*(A7), 6497–6513.

Werner, S., and G. W. Prölss (1997), The position of the ionospheric trough as a function of local time and magnetic activity, *Adv. Space Res.*, *20*, 1717–1722, doi:10.1016/S0273-1177(97)00578-4.

West, K. H., and R. A. Heelis (1996), Longitude variations in ion composition in the morning and evening topside equatorial ionosphere near solar minimum, *J. Geophys. Res.*, *101*(A4), 7951–7960.

Yizengaw, E., and M. B. Moldwin (2005), The altitude extension of the midlatitude trough and its correlation with plasmapause position, *Geophys. Res. Lett.*, *32*, L09105, doi:10.1029/2005GL022854.

Yizengaw, E., H. Wei, M. B. Moldwin, D. Galvan, L. Mandrake, A. Mannucci, and X. Pi (2005), The correlation between mid-latitude trough and the plasmapause, *Geophys. Res. Lett.*, *32*, L10102, doi:10.1029/2005GL022954.